

## Numerical study of pulsatile blood flow in micro channels

A.G. Kanaris, A.D. Anastasiou, S.V. Paras

Laboratory of Chemical Process and Plant Design, Department of Chemical Engineering,  
Aristotle University of Thessaloniki, GREECE

Tel.: +30 2310 996174; Fax: +30 2310 996209; e-mail: *paras@auth.gr*

### ***Abstract***

Understanding of blood flow dynamics is very important for biomedical applications. Blood is a multiphase fluid - containing red blood cells (*RBC*) in plasma - that exhibits non-Newtonian behaviour. Due to apparent drawbacks when conducting experiments with blood (e.g. coagulation), the use of a *CFD* code to simulate the pulsatile flow in blood vessels seem to be a promising alternative approach.

In this study, blood flow inside a 600 $\mu$ m hydraulic diameter micro channel (typical arteriole dimensions) comprising a bifurcation, a common geometry encountered in the human arterial system. Pulsatile flow is applied on the inlet to mimic flow conditions in the human body. Simulations were performed for a non-Newtonian fluid and a Newtonian used as reference. A commercial *CFD* code is employed to investigate the velocity distribution of blood in the micro channel and the wall shear stress as well as their modulation during the pulse. The comparison of the *CFD* data with the experimental findings reveals that the code predictions are highly reliable. The assumption of the Newtonian behavior of blood does not hold true for relatively low *Re* number flow in small blood vessels. Finally it was found that as it is reported for large arteries the shear stress on the outer wall are lower comparing with the stress on the inner wall and that makes it predisposed to plaque formation.

***Keywords:*** *Numerical study, non-Newtonian flow, pulsatile flow, arterioles, wall shear stress*

### ***Introduction***

Hemodynamic forces seem to have significant importance in biomechanical studies and medicine. Studying blood velocity distribution in arteries can be proved very useful in designing implantable devices, while it can help to make the choice between surgical and interventional procedures (Thiriet, 2007). In the relevant literature is reported (Chatzizisis and

Giannoglou, 2006; Shaaban and Duerinckx, 2000) that local hemodynamic forces affect the generation and the progression rate of atherosclerosis and that the atherosclerotic plaques develop mainly in regions of curvature, bifurcation, and branching of the blood vessels. A low wall shear stress promotes the formation of atherosclerotic plaque (Chatzizisis and Giannoglou, 2006), while, on the other hand, high shear stresses can cause the release of nitric oxide and prostacyclin which act as vasodilators and can protect the endothelial cells (John, 2009). Wall shear stress mapping may someday become part of the multifactorial, multidisciplinary approach to the early detection of atherosclerosis. Ever since the importance of hemodynamic forces has been accepted, several works have been published concerning blood flow in arteries (Gijssen et al., 1999a; Gijssen et al., 1999b; Huo and Kassab, 2006; Riva et al., 1985).

Blood is a multiphase mixture of plasma, a Newtonian fluid, and three main cell types, namely red blood cells, platelets and leukocytes. Its chemical composition and particularly the red blood cells are responsible for viscoelastic properties of blood (Fournier, 2007). In vessels with diameter greater than  $300\mu\text{m}$ , blood can be regarded as a homogeneous mixture. However, under low shear stress conditions normal red cells in plasma form linear aggregates (rouleaux) which disrupt flow streamlines and greatly increase the apparent viscosity of blood. By increasing the shear rates these aggregates are progressively deformed and hence the apparent blood viscosity decreases to the asymptotic limit of  $3.5\text{cP}$  (Fournier, 2007). On the other hand, in vessels with diameters smaller than  $300\mu\text{m}$ , blood behaves as a heterogeneous mixture, because the red blood cells move towards the center of the vessel leaving the plasma at the near-the-wall region. As a result the viscosity changes dramatically along the diameter of the vessel. This is known as the *Fahraeus-Linquist* effect (Majhi and Usha, 1988). The viscoelastic properties of blood greatly affect its flow dynamics (Gijssen et al., 1999a). Finding an analogue fluid with the same viscoelastic properties (especially in the case of small tubes where *Fahraeus-Lindquist* effect takes place) is very difficult. Many researchers made the assumption that blood can be considered as Newtonian fluid, due to the high shear rates existing in large arteries (e.g. Long et al., 2000; Mabotuwana et al., 2007; Stamatopoulos et al., 2010) but Gijssen et al. (1999a) suggests that this is not accurate as the non-Newtonian behavior has a significant effects on the velocity distribution.

It is also known that in vivo the walls of blood vessels are not rigid. The effect of arterial wall elasticity on the flow is difficult to be studied experimentally, because materials that

match the elastic behavior of arteries accurately are not readily available. Even though in large arteries there is a significant change in vessel diameter during the pulse, in small vessels, i.e., arterioles, where the pressure change is greatly attenuated, it can be assumed that the change in diameter is not significant and that the walls are practically rigid.

Taking all these into account it is obvious that simulating *in vivo* flow conditions for *in vitro* experiments is a difficult task. The studying of blood flow *in vivo* is also difficult, because blood cannot be easily handled (e.g. it coagulates), while common velocity measuring techniques (i.e., Ultrasonic Velocimetry, Laser Doppler Anemometry and micro Particle Image Velocimetry) can only be used *in vitro*. Thus, in place of expensive and time consuming experiments, CFD simulations can be used for predicting the blood behavior in arteries. Numerous works have been published on the numerical study of the hemodynamics in blood vessels (e.g. Chen and Lu, 2004; Olufsen et al., 2000; Soulis et al., 2008; Stamatopoulos et al., 2010). *CFD* is widely used for simulating flow in pipes, although the reliability of the simulation results must be checked against experimental data. The purpose of this study is to explore the potential of using a general purpose *CFD* code to compute the characteristics of blood flow in the bifurcation part of a small artery, by simulating experiments conducted previously in our Laboratory and comparing the results for validation. Moreover, a comparison will be made between the Newtonian and non-Newtonian behavior of blood in small tubes (arterioles) for relative low Reynolds number, and the effect of the viscoelastic properties on the wall shear stress during a full pulse.

### ***Experimental procedure***

The *scope* of the experimental study was to measure the velocity distribution of a blood analogue fluid in a bifurcation which is considered high risk geometry. The wall shear stress as well as its variation between two consecutive pulses was calculated from the velocity data. With the aim of simulating *in vivo* flow conditions, the following experimental conditions have been employed:

- An aqueous glycerin solution containing a small amount of xanthan gum simulates the viscoelastic properties of blood.
- The flow is pulsatile.
- The walls of the micro channel are rigid.

The non Newtonian behavior of human blood was simulated using an analogue which comprises 75% w/w distilled water, 25% w/w glycerin and xanthan gum (cause of the non-Newtonian behavior of the fluid). The viscosity of this solution was measured by a viscometer (*G1253-1006, Sigma-Alorich*). In **Figure 1** the viscosity of the blood analogue is compared with the viscosity of real blood given by Shin & Keum (2004) and with **Herschel-Bulkley** model (**Eq. 1**) which was used for viscosity prediction during *CFD* simulations. For shear rates ranging from 1 to 1000s<sup>-1</sup> the viscosity of the blood analogue employed is in very good agreement with blood viscosity. The standard error of fit for the **Herschel-Bulkley** model is estimated to be less than 6%. As reference to the Newtonian behavior an aqueous solution of glycerin with viscosity same with the asymptotic viscosity of blood (3.5cP), was employed (62% w/w distilled water and 38% w/w glycerin).

$$\mu = \frac{\tau_y}{\lambda\gamma} + K(\lambda\gamma)^{(n-1)} \quad (1)$$

where  $\mu$ : dynamic viscosity

$\tau_y$ : yield stress 0.02160 (Pa)

$\lambda$ : time constant 1 (s)

$\gamma$ : shear rate - (s<sup>-1</sup>)

$K$ : viscosity consistency 0.01345 (Pa s<sup>1/c</sup>)

$n$ : power law index 0.7812

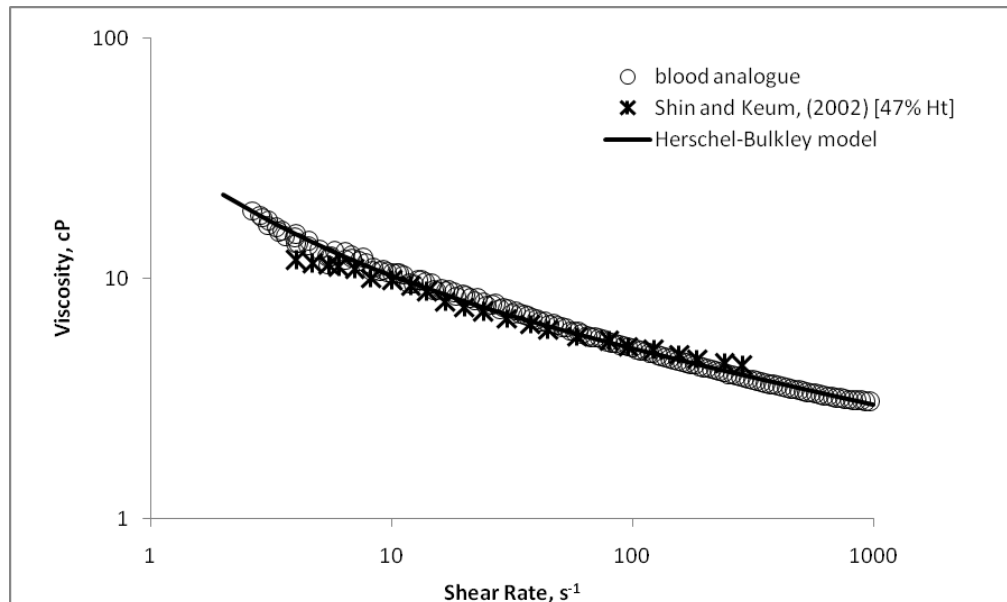


**Figure 1:** Comparison of viscosity between real blood, the blood analogue and the model used for the simulations.

Aiming to mimic physiological flow conditions pulsatile flow is generated using a syringe-pump (Alladdin, AI-2000), with upper limit at 340ml/hr and down limit at 140ml/hr (**Figure 2**). The pulse frequency is 1Hz, a rate that corresponds to 60 heart strokes per minute. For these flow conditions the Reynolds ( $Re$ ) number ranges from 9 to 21. An important quantity to be taken into account in pulsatile flow is Womersley number, which is the ratio of transient inertia over viscous forces and is defined as  $\alpha = R\sqrt{\omega\rho/\mu}$ , where  $\omega$  is the angular frequency,  $\rho$  the density and  $\mu$  the dynamic viscosity. For the present study Womersley number retains a constant value ( $\alpha=0.42$ ), because both the diameter of the micro channel and the frequency of the pulse are constant.

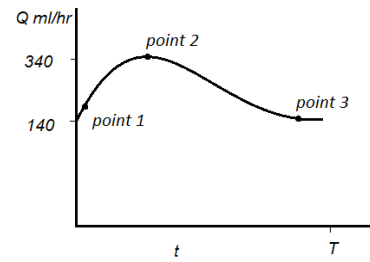


**Figure 2:** Pulse generated for the experiments.

All experiments were conducted in a 600 $\mu$ m hydraulic diameter micro channel (matching arteriole dimensions) comprising a bifurcation, manufactured by laser ablation in a polymeric chip and sealed with the same material. A micro channel with trapezoid cross section was used as a reasonable approximation since this is not far from the asymmetric geometry of human arteries (**Figure 3**) (Ford et al., 2001). The velocity data were acquired from the middle plane of the bifurcation, i.e., 300 $\mu$ m over the channel bottom.

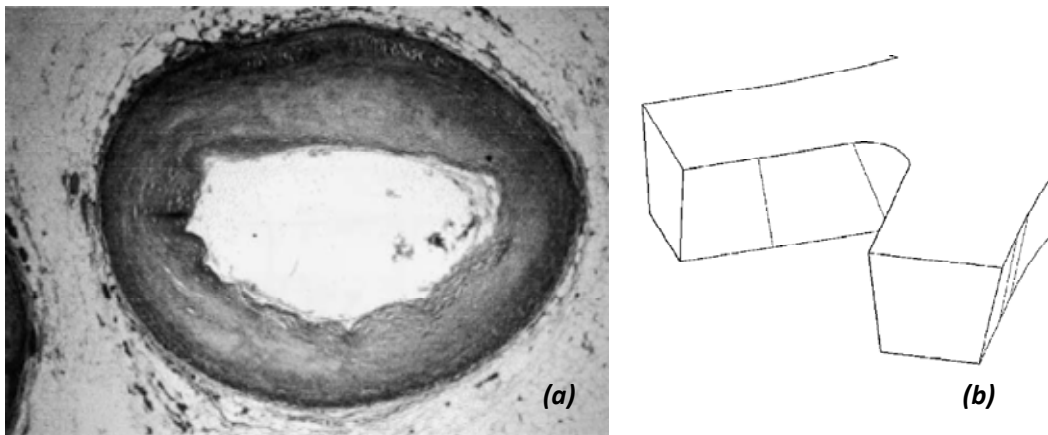


**Figure 3:** a) Cross section of healthy human artery; b) Cross section of the micro channel.

A backlight  $\mu$ -PIV system was used to study the flow. A micro strobe emitting at 532nm was used to illuminate the measurement section of the micro channel. The flow was recorded

with a high sense *CCD* camera (*Hisense MkII*, 1.4 Mpixel, 70% quantum efficiency), coupled to a Nikon microscope (*Eclipse LV100*). Polystyrene particles with mean diameter of 1 $\mu$ m were added to the fluids for tracing the flow. The image processing and the velocity estimation were performed using the *Flow Manager* Software (by *DantecDynamics*).

### ***Computational Procedure***

A commercial *CFD* code, namely *CFX*<sup>®</sup> 12.0, was employed to simulate accurately the experiments done in the laboratory in order to compare the results and validate the code. The bifurcation model was designed using images of the micro channel taken with the microscope (*Eclipse LV100*) for several depths (**Figure 4**).

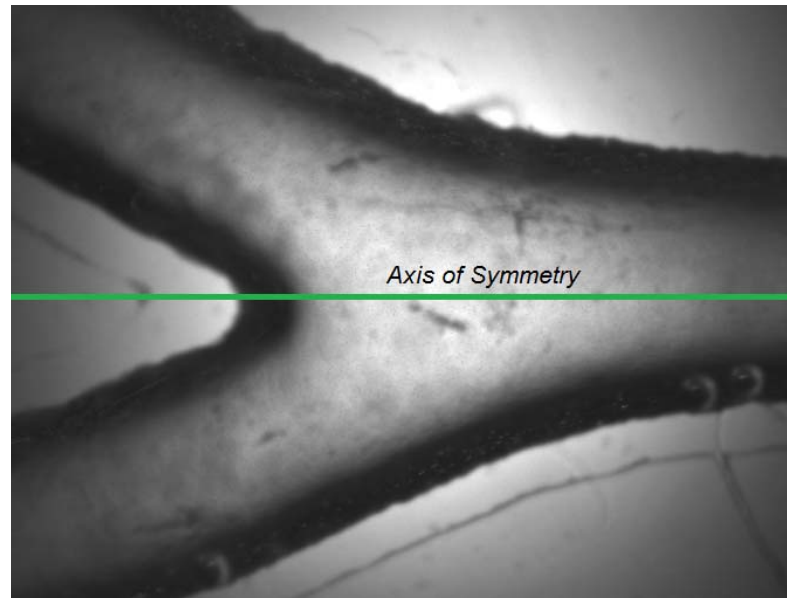


**Figure 4:** Microscope image of the middle plane of the bifurcation

After the dimensions of the bifurcation was determined, a model of the geometry was designed using a *CAD* program of *CFX*<sup>®</sup> 12.0 package. It is obvious that the flow is ***symmetrical*** with respect to the plane perpendicular to the plane of the bifurcation and is therefore adequate to perform the calculations only in one daughter tube and the corresponding part of the parent tube as shown in **Figure 5**.

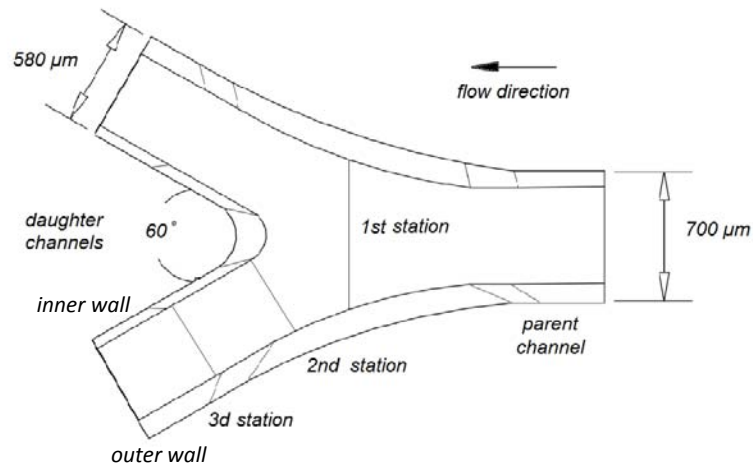


**Figure 5:** Dimensions of the micro channel.

Since it is known that the accuracy of the solution depends on the number and the size of the cells the final grid was chosen by a grid dependency study. Results of velocity distribution at the bifurcation for *Reynolds* number 50 was compared for four different grids (**Figure 6**). It was found that the solution becomes independent from the grid for 580,000 cells (same results with 660,000 cells) so the final grid comprises about 613,000 tetrahedral and prism elements (**Figure 7**). It must be noticed that the numerical study was employed for  $Re=21$  which is lower than the one used in the dependency study ( $Re=50$ ).

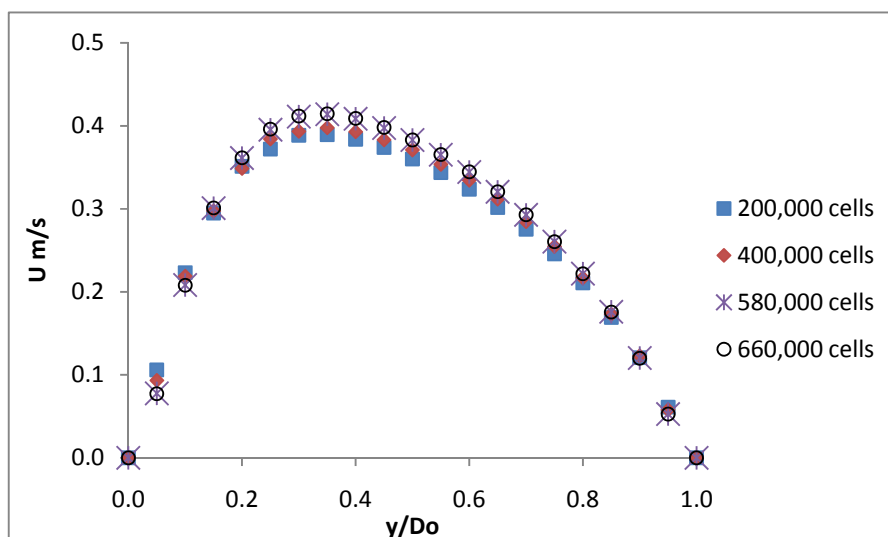


**Figure 6:** Dependency study for four different grids (velocity profile at the entrance of the bifurcation).

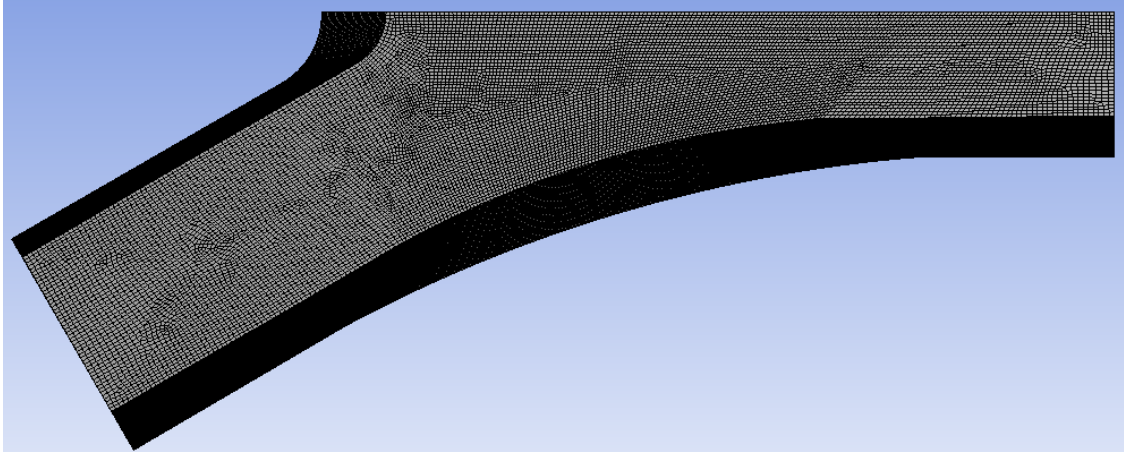


**Figure 7:** Grid used in the *CFD* simulations.

In order to simulate the viscoelastic behavior of the blood analogue and Newtonian fluid two new “*materials*” were created. The first one which simulates the blood analogue is non-Newtonian and follows a ***Herschel-Bulkley*** model (*Eq. 1*) and the second one is Newtonian with constant viscosity at 3.5cP.

Since the experiments conducted under pulsatile flow conditions, transient mode has been used for the simulation. The time step for each simulation is adjusted to 0.05s so as to limit the necessary number of calculation step for the time-consuming transient simulations. In order to simulate pulsatile flow conditions, a  $\sigma^{th}$  order polynomial was fitted to the experimental velocity data in the entrance of the parent tube and was used as the inlet boundary condition (**Figure 8**). The Direct Numerical Simulation (*DNS*) was applied since the *Re* is low and laminar flow is expected.

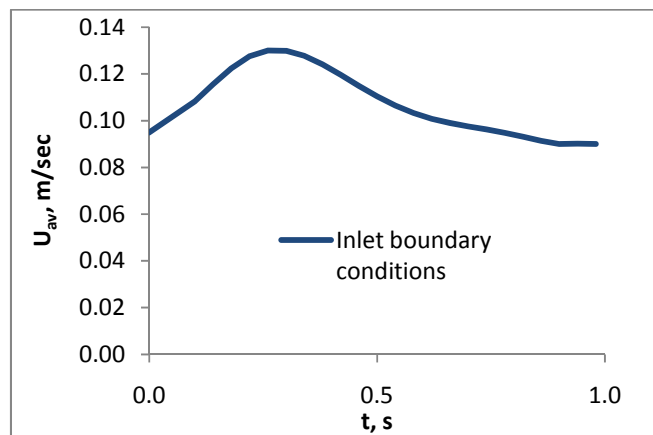


**Figure 8:** Expression of average velocity used as the inlet boundary condition.

Because of the increased computational demand and the numerous simulations needed, a high performance cluster (*HPC*) for parallel computations consisting of eighteen processors and 16GB RAM running a customized Gentoo Linux was used.

### **Results**

For the flow conditions of the experiments it was observed that at *station 2* the position of the maximum axial velocity is shifted towards the inner channel wall. It is well known that in curved conduits, transverse secondary flows arise as a result of the interplay between centrifugal and viscous forces. Since the driving centrifugal force depends quadratically on the average velocity, while the viscous force depends linearly on average velocity, secondary flows are strongly suppressed for low velocities. According to Paras (1979), who conducted experiments to simulate flow in human airways, for  $Re < 30$  the secondary flow decays before the first diameter downstream the bifurcation. This is verified by observing **Figure 9**, where the maximum velocity is shifted towards the inner wall after entering the bifurcation (*station 2*) and returns to the initial parabolic profile after a length of *one* diameter (*station 3*).

In **Figure 10** there is a comparison between experimental results and simulation data of the velocity distribution for the Newtonian fluid at *station 2*. The velocity data are normalized with respect to the maximum velocity. As it can be seen there is a good agreement between simulation and experiment during all the instants of the pulse. The same good agreement is observed and for the case of the non-Newtonian fluid as it is shown in **Figure 11**, where there is a comparison between experimental and simulation results for the non-Newtonian fluid. Same as before the velocity data are normalized with respect to the maximum velocity. Accordingly to these, it seems that *CFD* can accurately predict the flow dynamics both for Newtonian and non-Newtonian fluid. It is a logical conclusion that the results of the simulations are reliable and that *CFD* code can be used for the further study of similar systems without the need of more experiments.

After validating the code, a comparison between Newtonian and non-Newtonian behavior have been made. In **Figure 12** velocity data are presented at *station 2* for the two fluids during three different instants of the pulse. It is obvious that the velocity distributions are different. For the Newtonian fluid the maximum velocity is shifted from the centerline towards the inner wall of the bifurcation, during the whole pulse cycle. This displacement is not that intense in the case of non-Newtonian fluid, which returns to a parabolic profile at the end of pulse.

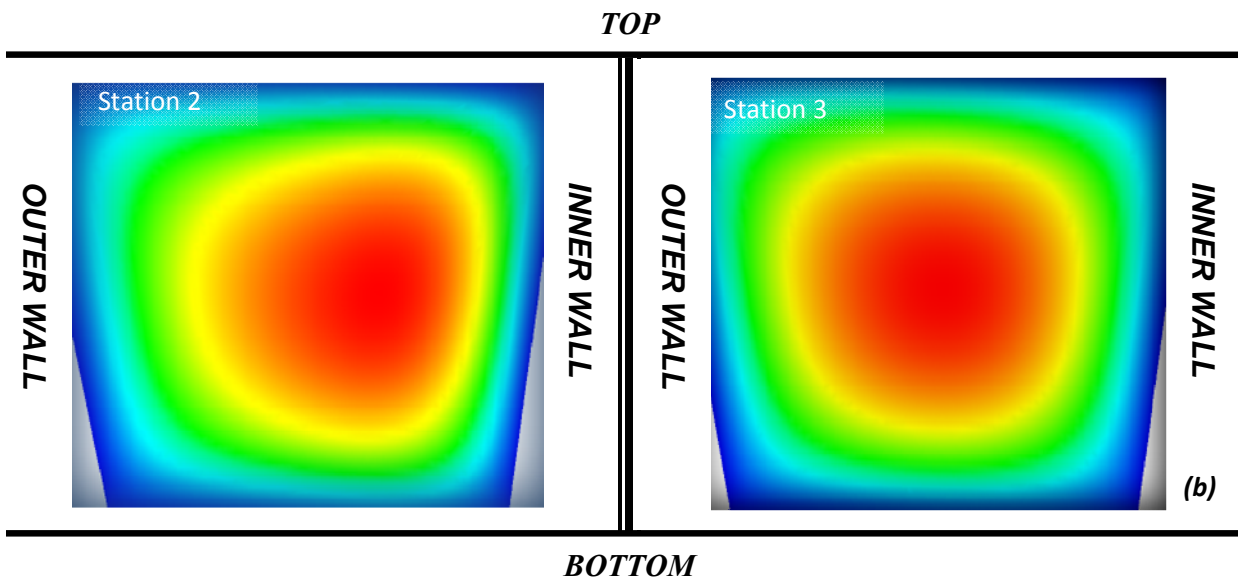
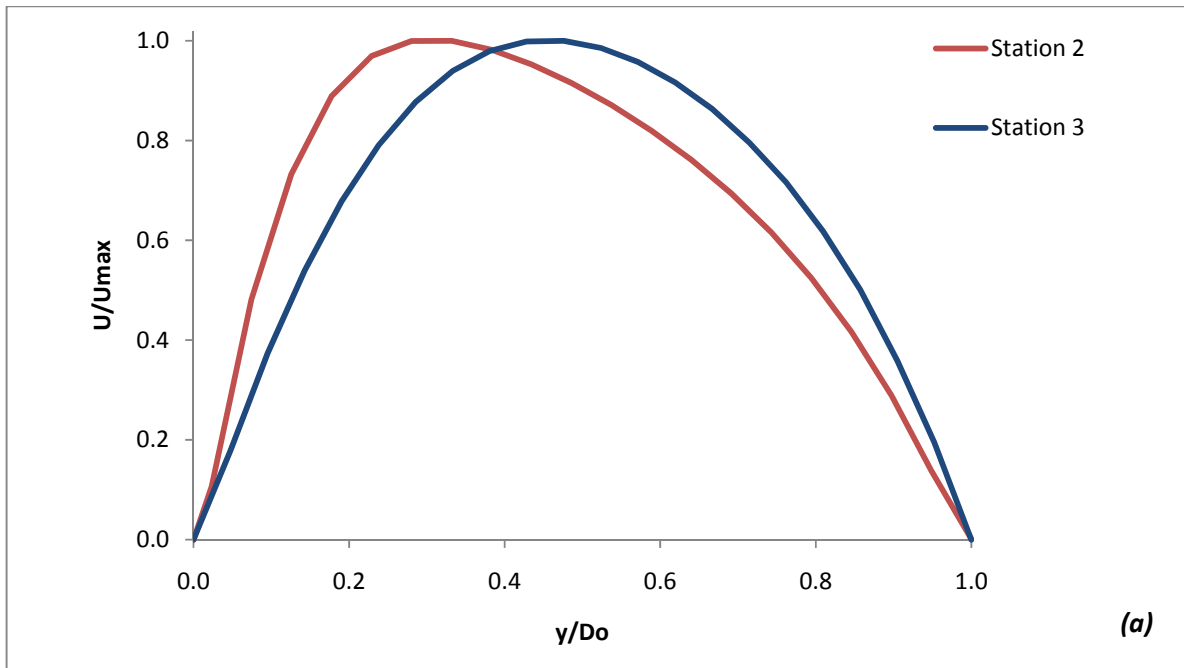


**Figure 9:** a) Velocity profiles at *stations* 2 and 3 for the Newtonian fluid b) Velocity contours on the plane perpendicular to the main flow at *stations* 2 and 3 for the Newtonian fluid.

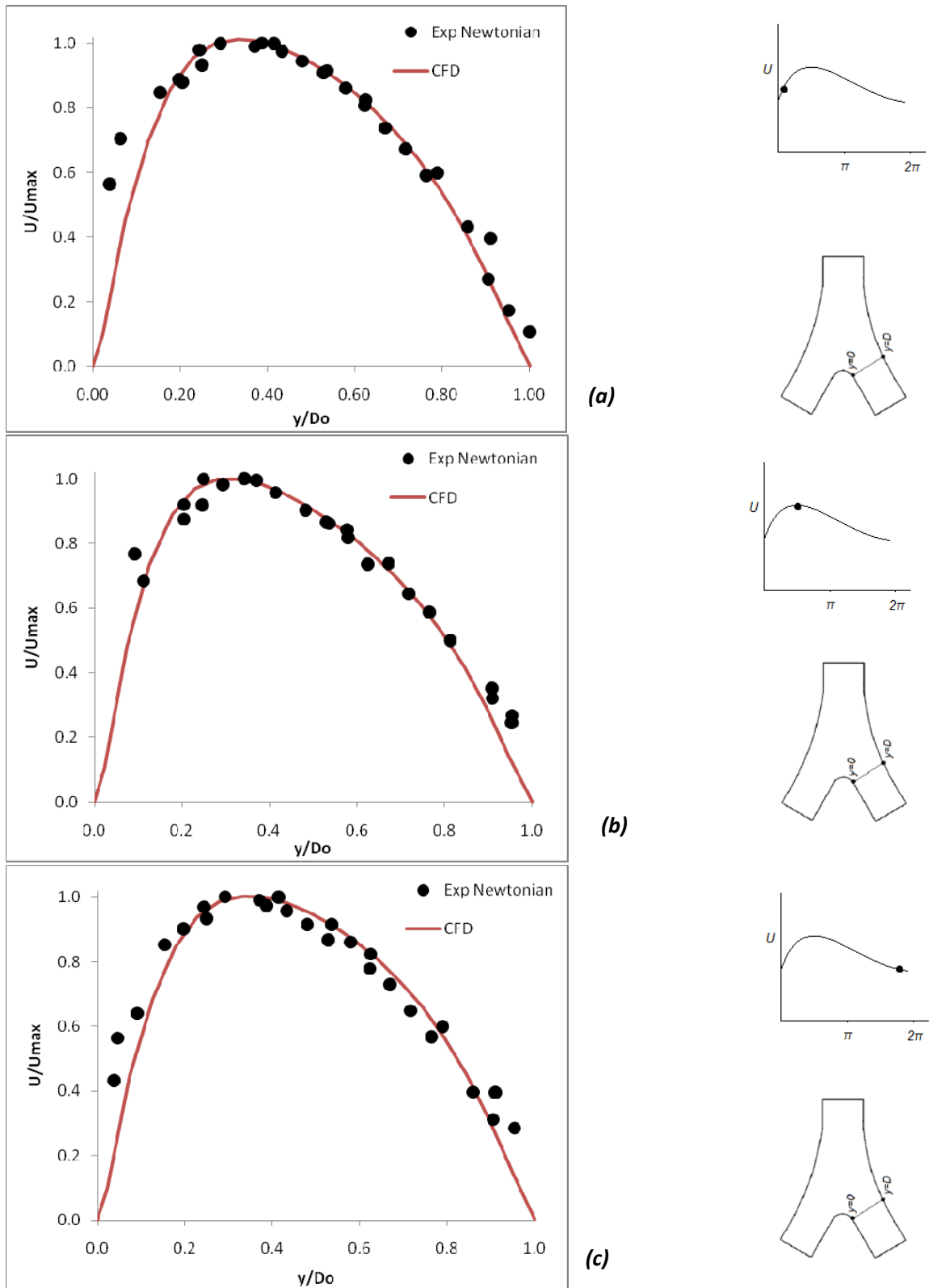


**Figure 10:** Comparison between *CFD* data and experimental results for the Newtonian fluid.

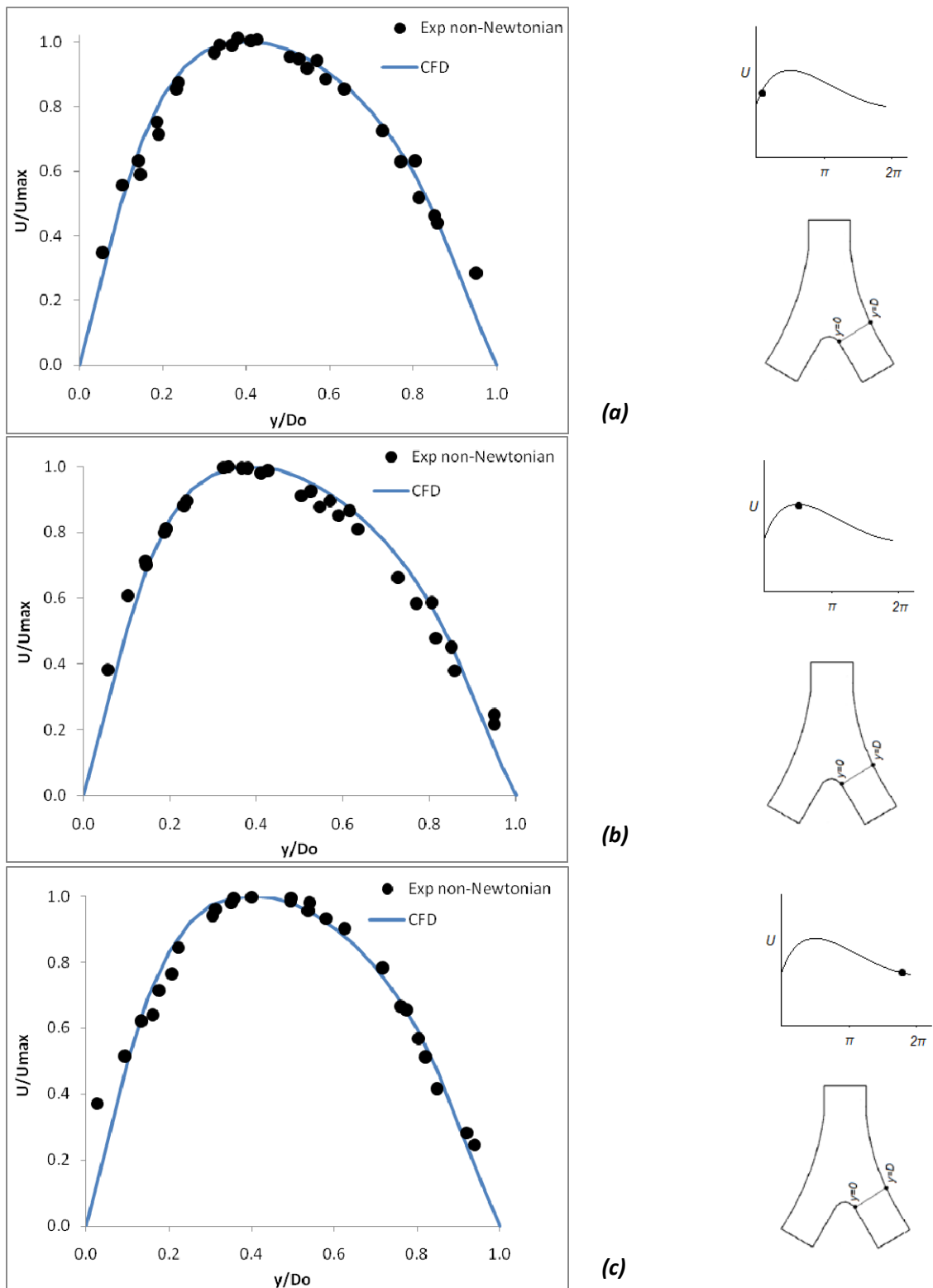


**Figure 11:** Comparison between *CFD* data and experimental results for the non-Newtonian fluid.

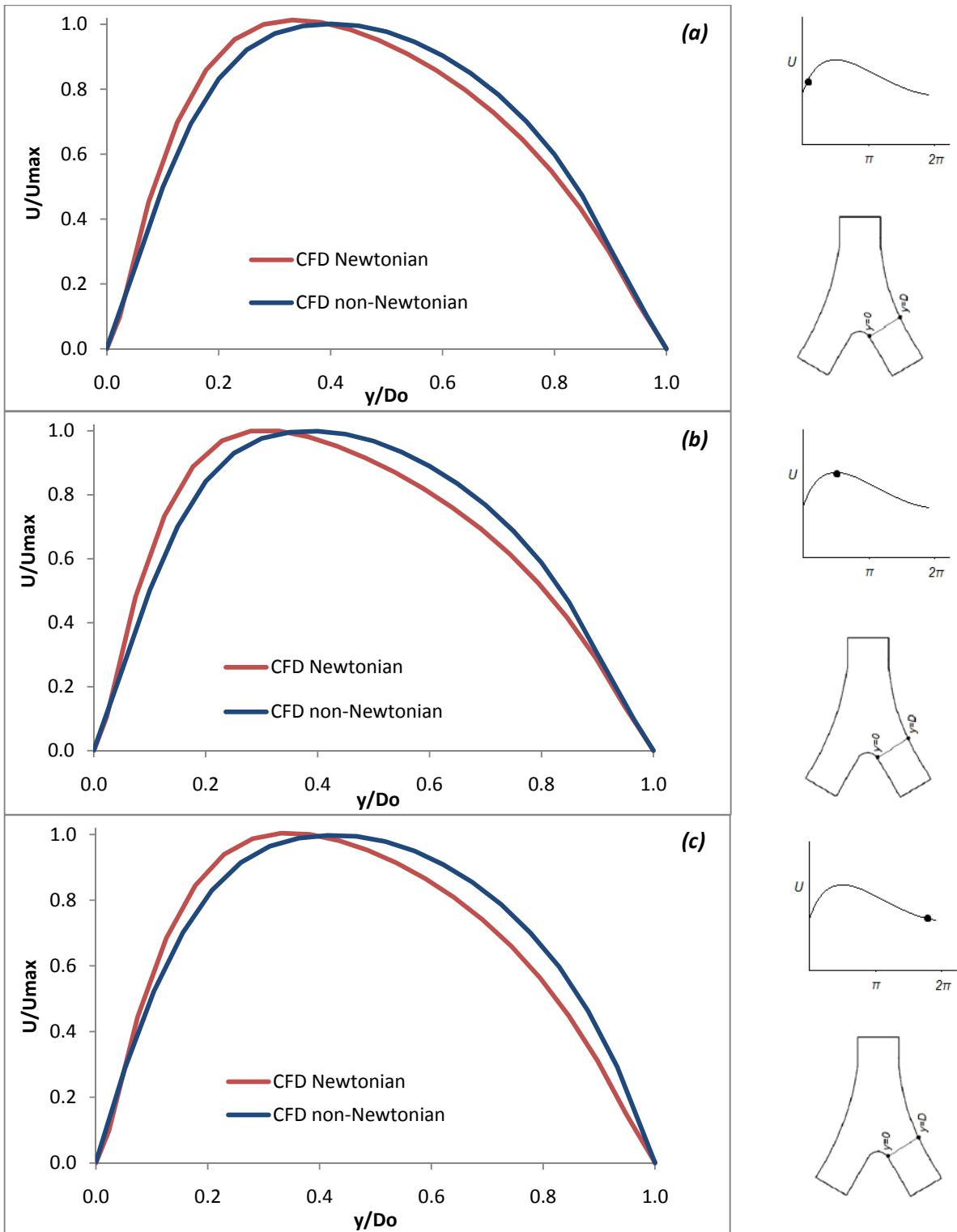


**Figure 12:** Comparison between Newtonian and non-Newtonian behavior from *CFD* data.

In **Figure 13** there is a comparison between the estimated wall shear stresses from the experimental results and the calculated from the *CFD* simulations. The data refers to the inner wall of the bifurcation at *station 2* and are normalized with respect to the maximum shear stress of the *Newtonian fluid* ( $\tau_{wmax}$ ). As it is obvious there is a good agreement between experimental and simulation results for both the Newtonian and the non-Newtonian fluids. Moreover, it is observed that both in the experiments and the simulations the wall shear stress for the Newtonian fluid is overestimated comparing with the non-Newtonian. The difference ranges between 30-40% depending on the instant of the pulse.

In **Figure 14** the difference between the estimated dimensionless wall shear stress for the inner and the outer wall for the two fluids is shown. In both cases the stresses on the outer wall are lower and that makes this area predisposed to plaque formation. A characteristic wall shear stress profile for the inner and the outer wall is presented in **Figure 15**. It is clear that the shear stresses on the outer wall are lower than these on the inner.

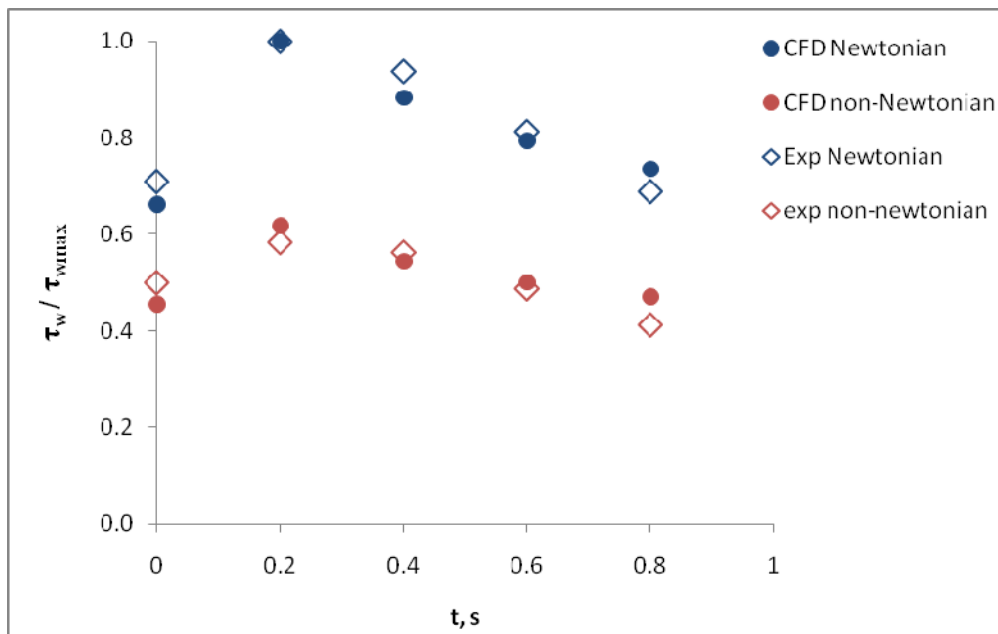


**Figure 13:** Comparison of inner wall shear stresses between experimental results and simulation data for the Newtonian and non-Newtonian fluid.

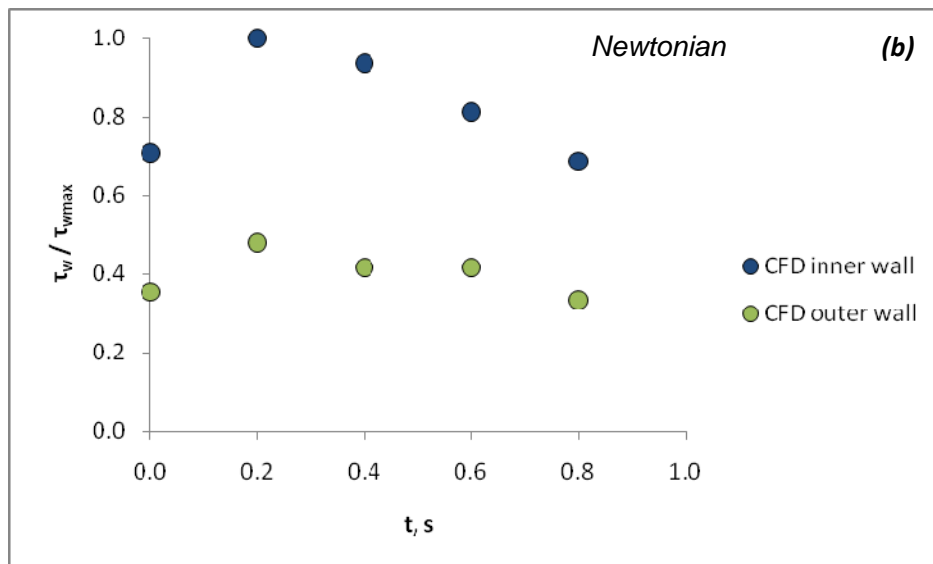
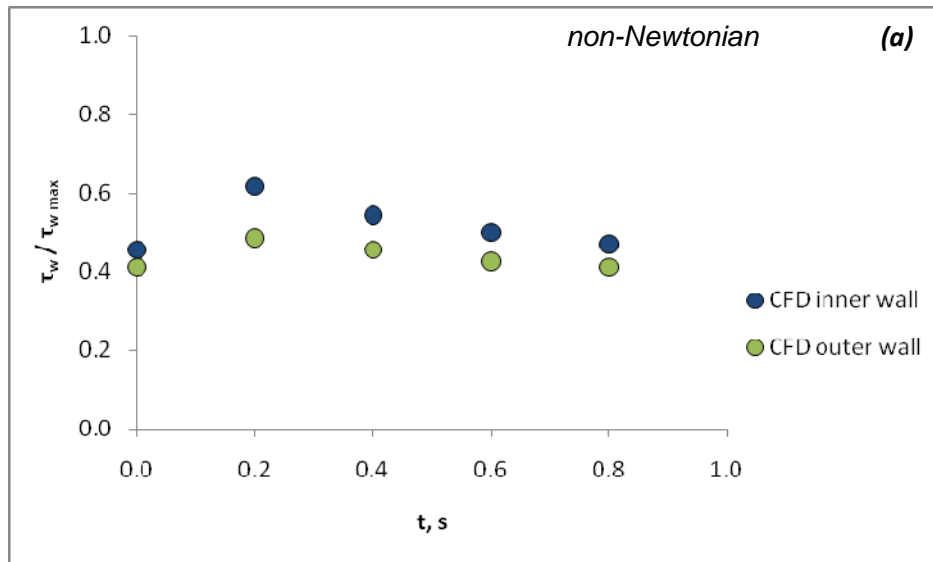
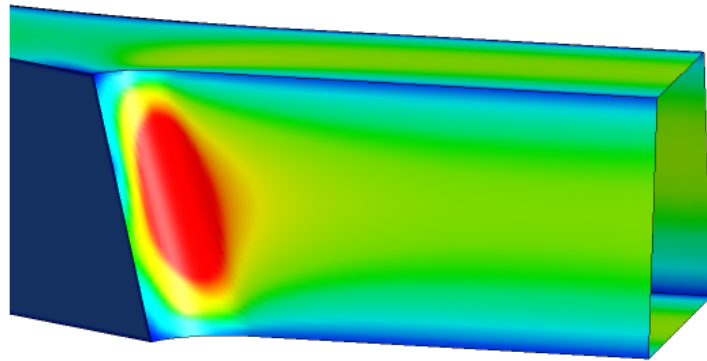
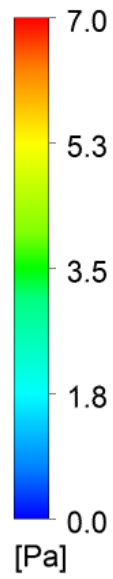
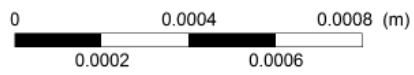


**Figure 14:** Comparison of wall shear stresses on the inner and the outer wall of the bifurcation a) for the non-Newtonian fluid b) for the Newtonian fluid.

Wall Shear Stress

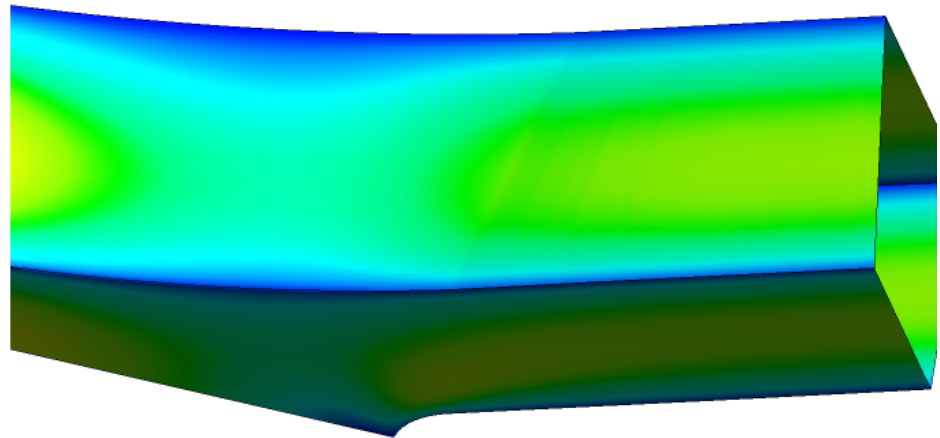
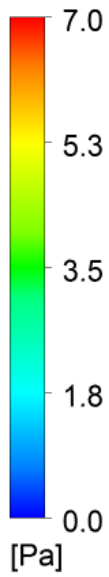


*Inner Wall*

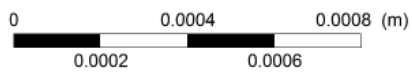


(a)

Wall Shear Stress



*Outer Wall*



(b)

**Figure 15:** Characteristic profile of wall shear stresses: a) on the inner wall of the bifurcation  
b) on the outer wall of the bifurcation.

## **Conclusion**

The scope of this work was the validation of a general purpose *CFD* code for the flow of a Newtonian and non-Newtonian fluid in a micro channel. The comparison of the *CFD* data with the experimental findings reveals that the code predictions are highly reliable. To summarize:

- *CFD* code was successfully validated and proved to be a useful tool for predicting pulsatile blood flow in small arteries.
- The velocity profiles of the two fluids tested for both cases studied (high and low flow rates), as expected, are different. At the entrance of the bifurcation the maximum of the profile is shifted towards the inner wall of the vessel and thus the shear stresses there are much higher than those on the outer wall. This is in agreement with relevant studies in larger human arteries and it means that the outer wall of an arteriole is more vulnerable to atherosclerosis than the inner one.
- It must be noted that the use of the Newtonian fluid gives rise to **higher** wall shear stress values (30 to 40%) in the bifurcation.

In conclusion, the assumption of the Newtonian behavior of blood does not hold true for relatively low *Re* number flows in small blood vessels. It is also verified that the shear thinning behavior of blood significantly affects the velocity profiles and consequently the wall shear stress and the hemodynamic forces. The role of the latter is crucial in understanding, diagnosis and treatment of cardiovascular diseases.

**Acknowledgments:** The authors wish to thank Prof. G.D. Giannoglou and Prof. J.V. Soulis for their helpful comments and suggestions.

## **References**

- Chatzizisis, Y. S. & Giannoglou, G. D. 2006. Pulsatile flow: A critical modulator of the natural history of atherosclerosis. *Medical Hypotheses*, 67, 338-340.
- Chen, J. & Lu, X.-Y. 2004. Numerical investigation of the non-Newtonian blood flow in a bifurcation model with a non-planar branch. *Journal of Biomechanics*, 37, 1899-1911.
- Ford, J. C., O'Rourke, K., Veinot, J. P. & Walley, V. M. 2002. The histologic estimation of coronary artery stenoses: Accuracy and the effect of lumen shape. *Cardiovascular Pathology*, 10, 91-96.
- Fournier, R. L. 2007. *Basic Transport Phenomena in Biomedical Engineering*, New York, Taylor & Francis Group, LLC.
- Gijssen, F. J. H., Allanic, E., Van De Vosse, F. N. & Janssen, J. D. 1999a. The influence of the non-Newtonian properties of blood on the flow in large arteries: unsteady flow in a 90° curved tube. *Journal of Biomechanics*, 32, 705-713.

- Gijssen, F. J. H., Van De Vosse, F. N. & Janssen, J. D. 1999b. The influence of the non-Newtonian properties of blood on the flow in large arteries: steady flow in a carotid bifurcation model. *Journal of Biomechanics*, 32, 601-608.
- Huo, Y. & Kassab, G. S. 2006. Pulsatile blood flow in the entire coronary arterial tree: theory and experiment. *Am J Physiol Heart Circ Physiol*, 291, H1074-1087.
- John, L. C. H. 2009. Biomechanics of Coronary Artery and Bypass Graft Disease: Potential New Approaches. *The Annals of Thoracic Surgery*, 87, 331-338.
- Long, Q., Xu, X. Y., Ariff, B., Thom, S. A., Hughes, A. D. & Stanton, A. V. 2000. Reconstruction of blood flow patterns in a human carotid bifurcation: A combined CFD and MRI study. *Journal of Magnetic Resonance Imaging*, 11, 299-311.
- Mabotuwana, T. D., Cheng, L. K. & Pullan, A. J. 2007. A model of blood flow in the mesenteric arterial system. *BioMedical Engineering OnLine*.
- Majhi, S. N. & Usha, L. 1988. Modelling the Fahraeus-Lindqvist effect through fluids of differential type. *International Journal of Engineering Science*, 26, 503-508.
- Olufsen, M. S., Peskin, C. S., Kim, W. Y., Pedersen, E. M., Nadim, A. & Larsen, J. 2000. Numerical Simulation and Experimental Validation of Blood Flow in Arteries with Structured-Tree Outflow Conditions. *Annals of Biomedical Engineering*, 28, 1281-1299.
- Paras, S. V. 1979. *Secondary flow near bifurcations at low Reynolds numbers*. MSc Thesis, University of Washington.
- Riva, C., Grunwald, J., Sinclair, S. & Petrig, B. 1985. Blood velocity and volumetric flow rate in human retinal vessels. *Invest. Ophthalmol. Vis. Sci.*, 26, 1124-1132.
- Shaaban, A. M. & Duerinckx, A. J. 2000. Wall Shear Stress and Early Atherosclerosis: A Review. *Am. J. Roentgenol.*, 174, 1657-1665.
- Shin, S. & Keum, D.-Y. 2002. Measurement of blood viscosity using mass-detecting sensor. *Biosensors and Bioelectronics*, 17, 383-388.
- Soulis, J. V., Giannoglou, G. D., Chatzizisis, Y. S., Seralidou, K. V., Parcharidis, G. E. & Louridas, G. E. 2008. Non-Newtonian models for molecular viscosity and wall shear stress in a 3D reconstructed human left coronary artery. *Medical Engineering & Physics*, 30, 9-19.
- Stamatopoulos, C., Papaharilaou, Y., Mathioulakis, D. S. & Katsamouris, A. 2010. Steady and unsteady flow within an axisymmetric tube dilatation. *Experimental Thermal and Fluid Science*, 34, 915-927.
- Thiriet, M. 2007. *Biology and Mechanics of Blood Flows Part II: Mechanics and Medical Aspects*, Paris, Springer.